Spectrum Defragmentation with Improved Lightpath Migration Scheme in Flex-grid Networks

Nguyễn Tuấn Khải, Ronald Romero Reyes, Thomas Bauschert
Technische Universität Chemnitz
Email: [tuan-khai.nguyen | ronald.romero-reyes | thomas.bauschert]@etit.tu-chemnitz.de

***Abstract*—The currently deployed fixed-grid Wavelength Division Multiplexing (WDM) technology is expected to be replaced by the more dynamic flex-grid WDM, which requires advanced methods for connection management and control (e.g., lightpath set-up and (re)configuration). The dynamic arrivals and departures of lightpaths often leave behind spectrum holes, causing fragmentation. In addition, reconfiguration of lightpaths often entails lightpath migrations that might cause disruptions of existing connections. Lightpath disruptions are expensive, as penalties will result as compensation for the violation of the service level agreements. In this paper, we analyze and identify the deficiencies of some existing work that tackles this problem. In particular, we show that the minimization of *High-slot Marks* might still lead to some fragmentation. Besides, these approaches neglect the lightpath configuration delays in the migration process. We develop optimization models that evidently better cope with these deficiencies. The performance improvements of the models are validated in a selected network scenario. The results also open up further research possibilities to better understand and model the trade-off between defragmentation gain and the degree of lightpath disruptions.**

***Index Terms*—flex-grid WDM, spectrum defragmentation, elastic optical networking, resource management in optical networks**

I. Introduction

With growing demand in traffic throughput, wavelength division multiplexing (WDM) networks require methods for automatic configuration of lightpaths. Fixed-grid WDM, with its moderate efficiency, has been deployed to handle this demand [1]. However, with more dynamic traffic, the operation of optical networks involves not only the establishment and teardown of optical connections, but also adjustments of existing configurations in an efficient way. A more recent technology—flex-grid WDM—is expected to take over from fixed-grid WDM due to its flexibility in bandwidth provisioning and spectrum management [2]. With narrow spectrum slots (around 12.5 GHz), flex-grid WDM can utilize the optical resources more efficiently.

Flex-grid WDM yet poses new challenges concerning connection management and control. The adoption of multiple discrete spectrum slots in flex-grid WDM usually leads to fragmentation of the optical spectrum [3]. This is caused by the dynamic arrivals and departures of lightpaths, leaving behind disjoint vacancies of different slot sizes in the spectrum. These spectrum holes, when summed up, are often sufficient to accommodate prospective connections, but their lack of contiguity leads to unnecessary rejections of new connection requests, causing severe underutilization of the optical resources. While the flex-grid WDM technology is capable of rectifying this fragmentation by shifting existing lightpaths across the spectrum, or even rerouting them, it remains algorithmically challenging as multiple lightpaths can span several different links. In addition, in order to maintain the operational costs within affordable ranges, the provisioning of lightpaths is subject to *spectrum contiguity* and *spectrum continuity* constraints. Furthermore, the task of reconfiguring lightpaths must take into consideration the interdependency among them, as spectrum assignments of lightpaths must not overlap. Since discrete states with multivariate interdependency are involved, this type of problem is well known to be $\mathcal{NP}$-hard [4].

Some recent work has been devoted to tackling this problem of spectrum defragmentation. Overall, there are two realms of approaches: nondisruption oriented and max-defragmentation oriented. The former forbids lightpath disruptions, so it might not yield optimal outcomes in terms of defragmentation. The latter focuses on the network fragmentation state with little or no attention to lightpath disruptions, so a lot of disruptions might result. For example, in [5], the authors look for new virtual topologies in order to maximize the carried traffic and avoid lightpath disruptions. In [6], virtual topologies are also adapted to load imbalances, but the idea of this reconfiguration is to disrupt existing lightpaths whenever necessary.

There is also research that seeks to balance the effects in these two aspects. Usually when lightpath disruptions are considered, one speaks of *seamless lightpath migration*, because this process involves the establishment of the new configuration before the teardown of the old (i.e., make-before-break approach). Failure to realize this order will result in a disruption. The idea is that once the target spectrum slots for a given lightpath are known to be currently occupied by other lightpaths, they need to be evacuated before being able to accommodate the lightpath in question. Jose and Somani in [7] introduce the *resource dependency digraph* (RDD) that exhibits the mutual dependency among lightpaths via their desired occupancy of spectrum slots, where each lightpath is represented by a vertex, and each directional arc indicates that the tail vertex requires spectrum slots currently occupied by the head vertex. Since the RDD is quite effective for its purpose, Takita et al in [8] adopt it and develop a mathematical model, named I-MWD (short for "Integer-Linear-Program-based

978-3-903176-33-1

Migration-integrated Wavelength Defragmentation"), to defragment the network spectrum while minimizing the number of lightpath disruptions. In the RDD, they associate each lightpath vertex with a so-called *acyclic hop count* (AHC) that helps to determine disruptions. For seamless migrations, the AHC value of the tail vertex must be greater than that of the head vertex. Violation of this condition will lead to a disruption. Ghallaj et al in [9] modify this model to yield better performance and name the new model MI-MWD (short for "Modified Integer-Linear-Program-based Migration-integrated Wavelength Defragmentation").

We also follow this pattern of using AHCs to assure as many seamless lightpath migrations as possible while minimizing the fragmentation state of the network. For this purpose, we adopt the concept of *fragmentation ratio*, defined in [10] as follows. Given a link s, the fragmentation ratio f_s of the link s is:

$$f_s = \frac{\text{number of allocation changes in link s}}{\text{number of spectrum slots in link s}} \qquad (1)$$

wherein "allocation change" refers to two adjacent spectrum slots in an optical link, one of which is occupied and the other is not. Fig. 1 shows four different links, each with six spectrum slots, together with the link fragmentation ratios on the right. The change in shade between two consecutive spectrum slots represents an allocation change. In this configuration, Link 4 has the lowest possible fragmentation ratio $\left(\frac{1}{6}\right)$, whereas Links 2 and 3 have the highest possible fragmentation ratios $\left(\frac{5}{6}\right)$.

Our contribution in this paper is to develop a mathematical model to optimize the fragmentation ratios of all links while taking into consideration the requirements of both spectrum contiguity and continuity for prospective lightpaths. We will show that regarding the fragmentation ratio alone might yield undesirable outcomes and that the additional consideration (both spectrum contiguity and continuity) further helps the spectrum defragmentation task. Furthermore, no work has really incorporated lightpath reconfiguration delays, hence underestimating the true penalty caused by possible disruptions due to lightpath migration clashes. In fact, this issue has also been discussed in [11], in which the authors aim to minimize the disruption time indirectly by means of minimizing the number of concurrent disruptions. We, on the other hand, target the disruption time more directly.

The rest of the paper is organized as follows. In Section II, several issues with the spectrum defragmentation task are discussed, followed by the construction of our novel mathematical models in Section III that cope with these issues. Section IV provides some performance evaluation of the new models. Section V gives a short summary of the paper and discusses future work.

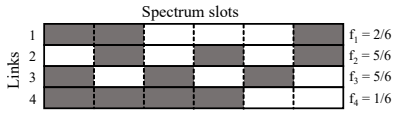

Fig. 1. An example of spectrum slot occupancy states of various optical links. The shaded areas are the occupied slots.

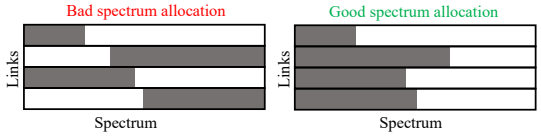

Fig. 2. An example of two spectrum mappings with identical fragmentation ratios but different occupancies. The shaded areas represent the occupied parts of the spectrum.

II. Problem Description

In this section, several issues encountered in the spectrum defragmentation approach by means of lightpath reconfiguration are described. To limit the complexity of the problem, we consider only existing optical connections and assume their routings remain unchanged. Defragmentation is therefore accomplished by shifting the existing occupancy of lightpaths across the spectrum slots.

A. Drawbacks of Solely Considering the Fragmentation Ratio

Part of the spectrum defragmentation task is to ensure both spectrum contiguity and continuity, especially for prospective lightpaths, so that the acceptance of new connections remains at a desirable rate. Spectrum continuity is the condition in which the spectrum slots occupied by one lightpath have to be identical across all the links that it spans. On the other hand, spectrum contiguity stipulates that spectrum slots belonging to the same connection be adjacent to each other.

Explicitly minimizing the fragmentation ratios can benefit spectrum contiguity, yet it has virtually no effect on spectrum continuity. Fig. 2 gives an example that illustrates such a case. The sum of fragmentation ratios is the same in both the spectrum assignment scheme on the left and on the right. However, the right scheme is preferable, since it is less likely to reject new lightpath assignment requests owing to better spectrum continuity for prospective lightpaths across the links.

As a way to address this issue, instead of directly applying fragmentation ratios as the main objective, Takita et al in [12] define a concept of high-slot mark (HM), which refers to the highest occupied spectrum slot index in a link. By minimizing the link HMs, lightpath assignments tend to the lower end of the spectrum in all links (similar to the configuration on the right in Fig. 2). However, we perceive that this approach still exhibits some drawbacks, as discussed in the following subsection.

B. Drawbacks of Solely Considering High-slot Marks

As discussed above, the issue of spectrum defragmentation is to be addressed using an objective function other than only the fragmentation ratios due to the fact that spectrum continuity should also be taken into consideration. By minimizing the HMs, the assignments of lightpaths are driven to one side of the spectrum. While Ghallaj et al in [9] have indeed proven the effectiveness of the use of HMs in the objective function of their mathematical model (MI-MWD),

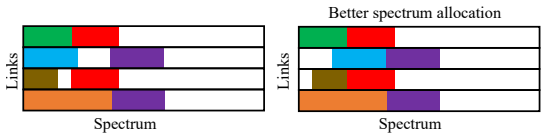

Fig. 3. An example of two spectrum mappings with identical HMs but different spectrum configurations. The colored areas represent the occupied parts of the spectrum.

Fig. 3 demonstrates the drawbacks of this approach. Here we color the occupied parts of the spectrum to underline the fact that defragmentation is primarily challenged by the requirements of both spectrum contiguity (horizontal occupancy, within a link) and spectrum continuity (vertical occupancy, across multiple links), where each color represents the assignment of a distinct lightpath. Two spectrum mappings (left and right) of identical HMs are shown. These mappings therefore would result to the same value of the objective function in MI-MWD. However, although all lightpath assignments in the mapping on the left are pushed to the lower side of the spectrum, we argue that this left mapping is less favourable, since it exhibits spectrum holes between occupied slots. In the mapping on the right, these holes are located at the lowest slots and hence they are more aligned with each other (note that alignment of vacancies is desirable for spectrum continuity). In addition, the mapping on the right would also yield better fragmentation ratios.

C. Consideration of Disruption Time

The resource dependency digraph (RDD) together with an acyclic hop count (AHC) assigned to each lightpath vertex is helpful in determining migration clashes (i.e., when two lightpaths are destined for the same spectrum slots). For seamless migrations, the RDD must be a *directed acyclic graph* (DAG) [13], in which case the AHCs will follow a *topological ordering*. However, defragmentation of spectrum by means of lightpath migration often entails a number of lightpath disruptions, in which case the RDD is no longer a DAG and hence contains at least one loop. This violation of the DAG constraint can be easily detected by failing to find a topological ordering for the AHCs.

Both [8] and [9] adopt this concept and add as a subordinate part of the objective function the number of lightpath disruptions, which is to be minimized. For each existing lightpath p, a binary variable $d^{(p)}$ is introduced, indicating whether p is disrupted (if $d^{(p)} = 1$) or not (if $d^{(p)} = 0$). The number of disruptions is then $\sum_{p \in P} d^{(p)}$, where P is the set of existing lightpaths. The AHC of each lightpath p is determined by a variable $ahc^{(p)}$, and the existence of an arc in the RDD from a lightpath $\tilde{p}$ to another lightpath p is governed by a binary variable $e^{(p,\tilde{p})}$. The following constraint is then used to mathematically model the RDD:

$$\mathcal{M} \cdot d^{(p)} + \mathcal{M} \cdot \left(1 - e^{(p,\tilde{p})}\right) - ahc^{(p)} + ahc^{(\tilde{p})} \geq m, \quad \forall (p, \tilde{p}) \in (P \times P) : p \neq \tilde{p} \qquad (2)$$

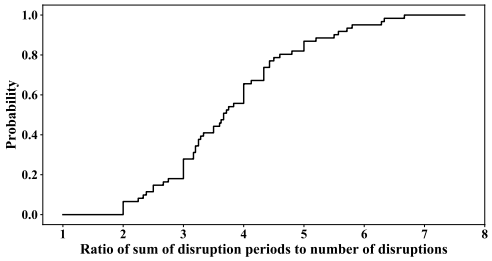

Fig. 4. Empirical CDF graph of the ratio of the disruption period to the number of disruptions when the MI-MWD model is applied.

wherein $\mathcal{M}$ and m are respectively a *Big-M* parameter and an infinitesimal parameter. Note that when an arc exists from $\tilde{p}$ to p (i.e., when $e^{(p,\tilde{p})} = 1$), seamless migration of p (i.e., $d^{(p)} = 0$) is only possible when $ahc^{(\tilde{p})} - ahc^{(p)} \geq m$, or equivalently, when $ahc^{(\tilde{p})} > ahc^{(p)}$. In other words, if this condition regarding the AHCs is not fulfilled, no topological ordering can be found and a lightpath disruption will result (i.e., $d^{(p)} = 1$).

However, since the variables $d^{(p)}$ are binary, this method minimizes the number of lightpath disruptions rather than the disruption periods. It has been shown that a reconfiguration step of a lightpath—even when it only involves shifting the spectrum occupancy—takes a while. According to [14], with state-of-the-art technologies, this reconfiguration time is about 70 seconds. Thus, by determining the number of reconfiguration steps during which a lightpath is disrupted, its disruption time in seconds can be inferred. Given the amount of time it takes to reconfigure a lightpath, disruption periods are probably more important than the number of disruptions in terms of service availability. With this consideration, using the $d^{(p)}$ variables as binaries could underestimate the true disruption periods. We run several tests on the MI-MWD model [9] to compute the ratio of the sum of disruption periods to the number of disruptions (using the binary variables $d^{(p)}$). Fig. 4 shows the empirical CDF graph of the results. As can be seen, most of the time the disruption periods are about two to seven times larger than merely the estimated number of disruptions. In other words, using only the number of disruptions does not closely reflect the true penalty caused by disruptions of lightpaths. In fact, it is also shown in [5] that the penalty fees are proportional to the disruption time, rather than the number of disruptions. More details on how the tests are conducted can be found in Section IV.

III. Novel Lightpath Migration Models

A. Objective-modified ILP-based Migration-integrated Wavelength Defragmentation (OMI-MWD)

The OMI-MWD model addresses the drawbacks of solely considering high-slot marks (HMs), which initially aims to solve the problem of spectrum defragmentation with both spectrum contiguity and continuity taken into consideration. In this new model, we omit the use of HMs and instead introduce a binary variable $\eta^{(s,w)}$ that dictates the presence of a spectrum

TABLE I
DEFINITIONS OF SETS AND PARAMETERS IN OMI-MWD

S	Set of optical fiber links
P	Set of existing lightpaths
ν	Number of spectrum slots in each link
b_p	Number of spectrum slots occupied by a lightpath p
w_p	Index of the first spectrum slot currently occupied by a lightpath p
I_s^p	Binary, 1 if lightpath p spans link s, 0 otherwise
$\mathcal{M}$	*Big-M* parameter
m	Infinitesimal parameter
α	Weight of the subordinate objective part

hole in link s, wherein the index w specifies the highest slot index the hole spans. We associate with each variable $\eta^{(s,w)}$ a weight of $(w+1)$ and minimize this weighted sum in the main part of the objective function, so as to either eliminate or drag any possible fragmentation holes to the lower end of the spectrum. The OMI-MWD model is listed as follows:

Minimize $$\sum_{s\in S}\sum_{w=0}^{\nu-2}(w+1)\cdot\eta^{(s,w)} + \alpha\cdot\sum_{p\in P} d^{(p)}$$

Subject to

C1: $$\sum_{w=0}^{\nu-1} x^{(p,w)} = 1, \quad \forall p \in P$$

C2: $$\sum_{p\in P} I_s^p \cdot \sum_{\tilde{w}=w-b_p+1}^{w} x^{(p,\tilde{w})} \leq 1, \quad \forall s \in S, w \in \{0,\ldots,\nu-1\}$$

C3: $$\sum_{w=w_p-b_{\tilde{p}}+1}^{w_p+b_p-1} x^{(\tilde{p},w)} = e^{(p,\tilde{p})}, \quad \forall s \in S, (p,\tilde{p}) \in (P\times P) : (p \neq \tilde{p} \wedge I_s^p = I_s^{\tilde{p}} = 1)$$

C4: $$\mathcal{M}\cdot d^{(p)} + \mathcal{M}\cdot\left(1 - e^{(p,\tilde{p})}\right) - ahc^{(p)} + ahc^{(\tilde{p})} \geq m, \quad \forall (p,\tilde{p}) \in (P\times P) : p \neq \tilde{p}$$

C5: $$\eta^{(s,w)} \geq \sum_{p\in P} I_s^p \cdot (x^{(p,w+1)} - x^{(p,w-b_p+1)}), \quad \forall s \in S, w \in \{0,\ldots,\nu-2\}$$

TABLE II
DEFINITIONS OF VARIABLES IN OMI-MWD

$x^{(p,w)}$	Binary—1 if w is the first spectrum slot occupied by a lightpath p, 0 otherwise
$\eta^{(s,w)}$	Binary—1 if slot $(w+1)$ of link s is occupied while slot w is not, 0 otherwise
$d^{(p)}$	Binary—1 if lightpath p is disrupted, 0 otherwise
$e^{(p,\tilde{p})}$	Binary—1 if lightpath $\tilde{p}$ occupies at least one spectrum slot currently occupied by lightpath p, 0 otherwise
$ahc^{(p)}$	Real non-negative—the AHC value of a lightpath p

TABLE III
EXPLANATION OF CONSTRAINTS IN OMI-MWD

C1	The first spectrum slot occupied by a lightpath must be unique.
C2	Each spectrum slot of a link can be occupied by at most one lightpath.
C3	Forces the variable $e^{(p,\tilde{p})}$ to 1 if the lightpath $\tilde{p}$ migrates to slots currently occupied by p, 0 otherwise.
C4	Ensures $ahc^{(\tilde{p})} > ahc^{(p)}$ if p is not disrupted when $e^{(p,\tilde{p})} = 1$.
C5	Forces $\eta^{(s,w)}$ to 1 if slot $(w+1)$ is occupied but slot w is not.

The meanings and definitions of sets, parameters, variables, and constraints used in OMI-MWD are listed in Tables I, II, and III. Note that Constraint C4 is the same as (2) from [8] and [9], as we still count the number of lightpath disruptions in the subordinate part of the objective function.

B. Disruption-and-Objective-modified ILP-based Migration-integrated Wavelength Defragmentation (DOMI-MWD)

To incorporate disruption periods (instead of number of disruptions), we redefine $d^{(p)}$ as integer variables and modify Constraint (2) into the following Constraint named C4-d:

C4-d: $$d^{(p)} + \mathcal{M}\cdot\left(1 - e^{(p,\tilde{p})}\right) - ahc^{(p)} + ahc^{(\tilde{p})} \geq 1, \quad \forall (p,\tilde{p}) \in (P\times P) : p \neq \tilde{p}$$

The primary difference between C4-d and (2) (or C4) is that the variable $d^{(p)}$ is no longer multiplied by a *Big-M* parameter, and that the right hand side is the value one, instead of an infinitesimal m parameter.

DOMI-MWD is almost the same as the OMI-MWD model outlined above (even the objective function is the same), with Constraint C4 replaced by C4-d. The variables $d^{(p)}$ now no longer indicate whether a lightpath is disrupted or not, but rather how long it is disrupted (i.e., its disruption period).

C. Disruption-modified ILP-based Migration-integrated Wavelength Defragmentation (DMI-MWD)

The DMI-MWD pertains to the mathematical model MI-MWD by Ghallaj et al in [9] that still uses HMs as the main objective for spectrum defragmentation. DMI-MWD only differs from MI-MWD in that Constraint (2) is replaced by C4-d and the variables $d^{(p)}$ are integers.

IV. PERFORMANCE EVALUATION

A. Scenario Setup

In this section, we report the performance of our models based on one scenario that involves the Abilene network from SNDLib [15] with 12 nodes and 15 links. We consider a network where all links are full-duplex and have the same set of 40 spectrum slots in both directions. This is also the test scenario used to generate the CDF graph in Fig. 4.

As for the optical connections, 70 traffic patterns are generated, each having a different number of node pairs, ranging from 10 to 79 pairs. Each node pair represents the two endpoints of a lightpath, which are selected randomly from

the set of all possible node pairs in the network. Moreover, to make the traffic patterns more realistic, out of the 12 nodes, we select three nodes with the highest *PageRank* [16] and increase their probabilities of being chosen as a lightpath endpoint by a factor of four. In other words, these three nodes are four times more likely than other nodes to be chosen as an endpoint of a lightpath. The lightpaths are routed using the shortest path algorithm [17] and occupy a certain number of contiguous spectrum slots, selected uniformly among the set $\{2, 4, 8\}$. To create a fragmentation state in the network, the spectrum slots are assigned using the random-fit spectrum allocation policy [18]. Moreover, in the objective function, the weight α is 0.01.

Each traffic pattern represents a problem instance, which then is solved using the OMI-MWD, DOMI-MWD, MI-MWD (in [9]), and DMI-MWD models (i.e., each problem instance is solved four times). The models are solved by a mixed integer programming (MIP) solver from CPLEX version 12.9 on an Intel i7-3930K machine with 6 cores at 3.2GHz. To restrict the computation time we set the time limit to 1.5 hours and the relative MIP gap tolerance to 2%.

B. Results

We compare OMI-MWD against MI-MWD in terms of the sum of fragmentation ratios of all links and show the results in Fig. 5. The blue line is the reference line (with slope 1), below which OMI-MWD outperforms MI-MWD and above which MI-MWD outperforms OMI-MWD for each traffic pattern. This is because each data point takes the sum of fragmentation ratios from MI-MWD as its x-coordinate and that from OMI-MWD as its y-coordinate. Data points that lie on the reference line show no difference between MI-MWD and OMI-MWD, as the x- and y-coordinates are equal in such cases. As can be seen, many data points lie below the reference line and very few are slightly above it.

To have more insight into the results, in Fig. 6 we exemplify two spectrum assignment mappings resulting from MI-MWD (on the left of Fig. 6) and OMI-MWD (on the right) for the same traffic pattern. As has been argued in Section II, the MI-MWD—with the use of HMs—drives the assignments of lightpaths to the lower end of the spectrum, but it might still leave random holes between occupied slots. Most of these

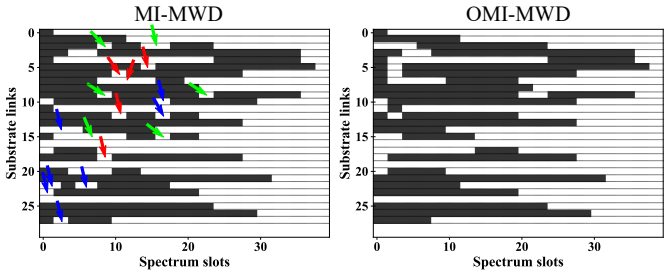

Fig. 6. An example of two mapping solutions of the same problem instance from MI-MWD (left) and OMI-MWD (right).

holes are indicated in Fig. 6 by the arrows, which contribute to the spectrum fragmentation. The OMI-MWD model targets these spectrum holes by either shifting them to the lower end so they are more aligned (the red arrows), merging them to make bigger holes so there are more contiguous vacancies (the green arrows), or eliminating them (the blue arrows). Naturally, due to certain constraints, the OMI-MWD model itself still exhibits some holes in the spectrum. However, since spectrum holes are tackled by the objective of the OMI-MWD model, they are minimized and hence yield better overall fragmentation outcomes, as compared to the MI-MWD model.

Fig. 7 illustrates the sum of disruption periods as the results of the MI-MWD model (the x-axis) against that of the DMI-MWD model (the y-axis). Again, the blue line in Fig. 7 is the reference line which marks the border between the region where DMI-MWD is better than MI-MWD (below the reference line) and the region where DMI-MWD is worse (above the reference line). Here we observe cases in which the DMI-MWD model yields slightly worse outcomes as compared to MI-MWD, but in very many cases we also observe a lot of improvement that DMI-MWD makes. Note that while the y-coordinates are computed simply by summing all the solutions for the $d^{(p)}$ variables, the x-coordinates are calculated in post-processing with the help of the *hierarchical RDD reconstruction* algorithm [12], as the variables $d^{(p)}$ in MI-MWD do not represent disruption time. The periods in Fig. 7 are not gauged in seconds, but this can be done by simply multiplying these values by 70 seconds (i.e., the average time

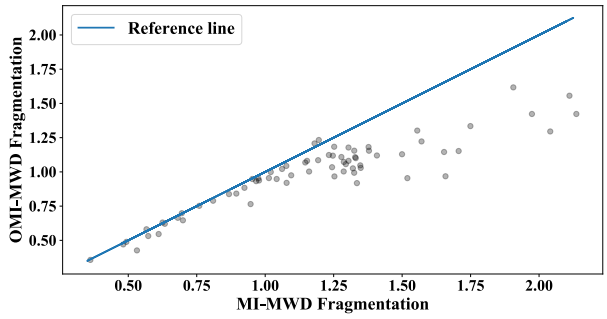

Fig. 5. Comparison between OMI-MWD and MI-MWD in terms of fragmentation ratios. Above the reference line: 3 points, below the reference line: 58 points, on the reference line: 9 points.

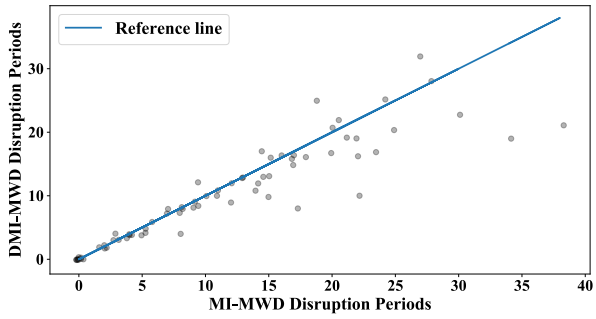

Fig. 7. Comparison between DMI-MWD and MI-MWD in terms of disruption periods. Above the reference line: 13 points, below the reference line: 38 points, on the reference line: 19 points.

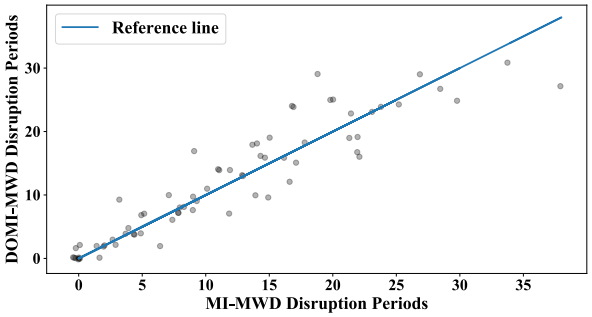

Fig. 8. Comparison between DOMI-MWD and MI-MWD in terms of disruption periods. Above the reference line: 25 points, below the reference line: 23 points, on the reference line: 22 points.

each configuration step takes [14]).

In terms of fragmentation ratios, the DOMI-MWD model produces quite similar results to the OMI-MWD model. The comparison of DOMI-MWD against MI-MWD in this aspect looks similar to Fig. 5. However, in terms of disruption periods, Fig. 8 shows that DOMI-MWD does not give any benefit as compared to MI-MWD, since there are comparable amounts of data points above and below the reference line. In fact, this is to be expected, as improvement in defragmentation (due to the modified objective function in the case of DOMI-MWD) often comes at the cost of increased lightpath disruptions. Therefore, the fact that DOMI-MWD can cause more disruptions shows that our new models are still subject to the trade-off between the minimization of defragmentation and disruption periods.

Apart from the Abilene network, other scenarios yield quite similar outcomes, whose results thus are not shown here.

V. Conclusion and Outlook

Defragmentation of optical network spectrum by means of lightpath reconfigurations has been made more flexible and dynamic thanks to the recent advent of flex-grid WDM. However, the reoptimization of the optical configurations is often accompanied by migrations of lightpaths, which in effect might result in disruptions due to their mutual dependency on the occupancy of spectrum slots. In this paper, we revisit the concept of high-slot marks (HMs) that is used both to optimize the fragmentation ratios and ensure spectrum contiguity and continuity. We argue that this approach still leads to some fragmentation and therefore develop our own method to better address this issue. Moreover, understanding that the penalty caused by lightpath disruptions has more to do with the periods of disruptions than the number of disruptions itself, we redefine the variables pertaining to lightpath disruptions so that they reflect closer the penalty. Many test runs with several network scenarios have indeed proven that our new models outperform MI-MWD.

DOMI-MWD however does not give any benefit in terms of disruptions. For future work, we aim to tackle this trade-off between disruption and fragmentation. We observe that the formulation of the existing models still exhibits some implicit constraints that can be safely lifted. For instance, a lightpath, once migrated, is not allowed to migrate a second time. When this restriction is removed, multiple migration steps then need to be considered individually.

Acknowledgment

This work was performed in the framework of the Celtic-Plus project AI-NET-PROTECT, funded by the German BMBF (ID 16KIS1285).

References

[1] S. Talebi, F. Alam, I. Katib, M. Khamis, R. Salama, and G. N. Rouskas, "Spectrum management techniques for elastic optical networks: A survey," *Optical Switching and Networking*, vol. 13, pp. 34–48, 2014.

[2] I. Tomkos, S. Azodolmolky, J. Sole-Pareta, D. Careglio, and E. Palkopoulou, "A tutorial on the flexible optical networking paradigm: State of the art, trends, and research challenges," *Proceedings of the IEEE*, vol. 102, no. 9, pp. 1317–1337, 2014.

[3] J. Ahmed, F. Solano, P. Monti, and L. Wosinska, "Traffic re-optimization strategies for dynamically provisioned wdm networks," in *15th International Conference on Optical Network Design and Modeling-ONDM 2011*. IEEE, 2011, pp. 1–6.

[4] H. R. Lewis, "Computers and intractability. a guide to the theory of np-completeness," 1983.

[5] M. Saad and Z.-Q. Luo, "Reconfiguration with no service disruption in multifiber wdm networks," *Journal of lightwave technology*, vol. 23, no. 10, p. 3092, 2005.

[6] A. Gençata and B. Mukherjee, "Virtual-topology adaptation for wdm mesh networks under dynamic traffic," *IEEE/ACM Transactions on networking*, vol. 11, no. 2, pp. 236–247, 2003.

[7] N. Jose and A. K. Somani, "Connection rerouting/network reconfiguration," in *Fourth International Workshop on Design of Reliable Communication Networks, 2003.(DRCN 2003). Proceedings.* IEEE, 2003, pp. 23–30.

[8] Y. Takita, K. Tajima, T. Hashiguchi, and T. Katagiri, "Wavelength defragmentation with minimum optical path disruptions for seamless service migration," in *Optical Fiber Communication Conference*. Optical Society of America, 2016, pp. M2J–3.

[9] A. Ghallaj, R. R. Reyes, M. Ermel, and T. Bauschert, "Optimizing spectrum allocation in flex-grid optical networks," in *Photonic Networks; 18. ITG-Symposium*. VDE, 2017, pp. 1–8.

[10] Y. Yu, J. Zhang, Y. Zhao, H. Li, Y. Ji, and W. Gu, "Exact performance analytical model for spectrum allocation in flexible grid optical networks," *Optical Fiber Technology*, vol. 20, no. 2, pp. 75–83, 2014.

[11] F. Solano and M. Pióro, "Lightpath reconfiguration in wdm networks," *Journal of Optical Communications and Networking*, vol. 2, no. 12, pp. 1010–1021, 2010.

[12] Y. Takita, T. Hashiguchi, K. Tajima, T. Katagiri, T. Naito, Q. Zhang, X. Wang, I. Kim, P. Palacharla, and M. Sekiya, "Agile network re-optimization supporting seamless service migration," in *2015 Optical Fiber Communications Conference and Exhibition (OFC)*. IEEE, 2015, pp. 1–3.

[13] K. Thulasiraman and M. Swamy, "5.7 acyclic directed graphs," *Graphs: theory and algorithms*, vol. 118, 1992.

[14] R. Singh, M. Ghobadi, K.-T. Foerster, M. Filer, and P. Gill, "Radwan: rate adaptive wide area network," in *Proceedings of the 2018 Conference of the ACM Special Interest Group on Data Communication*, 2018, pp. 547–560.

[15] S. Orlowski, R. Wessäly, M. Pióro, and A. Tomaszewski, "Sndlib 1.0—survivable network design library," *Networks*, vol. 55, no. 3, pp. 276–286, 2010.

[16] I. Rogers, "The google pagerank algorithm and how it works," 2002.

[17] T. H. Cormen, C. E. Leiserson, R. L. Rivest, and C. Stein, *Introduction to algorithms*. MIT press, 2009.

[18] R. R. Reyes and T. Bauschert, "Reward-based online routing and spectrum assignment in flex-grid optical networks," in *2016 17th International Telecommunications Network Strategy and Planning Symposium (Networks)*. IEEE, 2016, pp. 101–108.